DEVELOPMENT OF A MICROPUMP FOR MICROELECTRONIC COOLING*

C. Channy Wong, and Douglas R. Adkins
Engineering Sciences Center
Sandia National Laboratories
Albuquerque, New Mexico 87185-0827

Dahwey Chu
Microelectronics and Photonics Center
Sandia National Laboratories
Albuquerque, New Mexico 87185-1082

ABSTRACT

To demonstrate a system integration process for Micro-Electro-Mechanical Systems (MEMS), we are building an active cooling MEMS unit for microelectronics applications. This integrated unit will incorporate a micropump, temperature sensors, microchannels, and heat exchange devices into a single unit. The first phase of this research project is to develop and test a micropump capable of moving the working fluid within the integrated device. This paper will discuss the design, development, testing, and evaluation of a micropump concept.

The micropump which was developed is an electrohydrodynamic (EHD) injection pump. Fabrication of the pump was accomplished using laser micromachining technology, and two initial designs were examined for full fabrication. The first design has two silicon parts stacked vertically on top of each other. Gold is deposited on one side of each stacked plate to serve as electrodes for the electrohydrodynamic pump. A Nd:YAG laser is used to drill an array of circular holes in the "well" region of both silicon parts, leaving an open pathway for fluid movement. Next the silicon parts are aligned and bonded together, thus becoming a EHD pump. Fluid flow has been observed when an electric voltage is applied across the electrodes. The second design has the silicon parts which contain the flow grid oriented "back-to-back" and bonded together. This "back-to-back" design has a shorter grid distance between the anode and cathode plates so that a smaller voltage is required for pumping. Preliminary results from laboratory experiments have demonstrated that this EHD micropump design can achieve a pressure head of about 287 Pa with an applied voltage of 120 V.

NOMENCLATURE

E_x, E_o	Electric field
J_f, J_o	Current density
L	Separation distance between electrodes
V	Applied voltage across electrodes
a	Radius of charged particles
b	Mobility of charged particles, $b=2\varepsilon_o aE_x/\mu$
d	Height of the rectangular conduit
v_x	Fluid velocity in x-direction
w	Width of the rectangular conduit
ε_o	Dielectric constant
μ	Viscosity of fluid
ρ_i	Charged particle density

*This work was supported by the United States Department of Energy under contract number DE-AC04-94AL85000 through the Laboratory Directed Research and Development (LDRD) program.

INTRODUCTION

The advances in silicon fabrication technology have led to the development of many micro devices and systems such as pressure and temperature sensors, micromotors, and microactuators. This new technology is commonly known as Micro-Electro-Mechanical Systems or MEMS. The characteristic length of these devices is on the order of a few microns. They can achieve high reliability and are relatively inexpensive to manufacture because they can be produced in large quantities.

Even though the MEMS silicon microstructure technology has been advancing rapidly over the past decade, most MEMS research has been focused on the fabrication and testing of single components. Very limited work exists in the integration of a number of different MEMS devices into a single engineering system. Building and testing such systems is a complex and difficult task often characterized by multiple iterations.

System Integration Process

The overall goal of our research program is to develop and demonstrate a reasonable process for system integration of micro devices. Our interest is to reduce the number of iterations between the design, fabrication, and testing process and to shorten the development-

to-production time. The basic approach to improving and hastening the system integration process is to incorporate computational modeling into the design loop and to include mechanical analysis in electrical design considerations at an early phase of the system development.

To demonstrate how the MEMS integration process would work, we are designing, building, and testing an active cooling system for microelectronics applications (Fig. 1). The integrated unit will have the following components: a field array of temperature sensors to locate local hot spots, thermally driven microactuators, micropumps and microchannels. This cooling system can be considered as a single loop micro-heat exchanger to remove heat from a hot spot region and reject heat at some other location where heating is less critical.

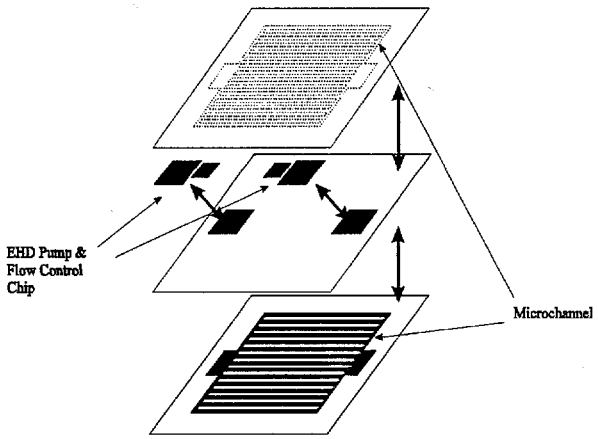

Figure 1 Schematic Diagram of an Active Cooling System.

Rapid Prototyping and Laser Micromachining

One critical component of the integrated cooling unit is the micropump which is responsible for moving the working fluid. It is very important to fabricate, test, and evaluate the micropump quickly and efficiently so that we can finalize the basic design early. After reviewing the existing fabrication processes for micromachines, we decided to fabricate a micropump based on the electrohydrodynamic principle using laser micromachining technology which would shorten the "research-to-development-to-production" cycle and save time.

Laser micromachining bridges the gap between the resolution obtainable by conventional mechanical machining operations and chemical micromachining techniques. Using conventional machining processes, it is extremely difficult, if not impossible, to produce machined components with structures several mils (1 mil ≈ 25 microns) in size with tolerances of a quarter of a mil. Chemical micromachining techniques allow much smaller structures (on the order of a few microns in size) to be produced; these techniques have limitations in the materials that can be machined and in obtaining high-aspect-ratio geometries. In general, chemical micromachining techniques are a planar technology and rely on isotropic etchants to remove the excess material. Thus, material is removed uniformly from the substrate in all directions. However, using a chemical micromachining process to develop and fabricate a conceptual micro device takes time and is relatively expensive.

For bulk micromachining processing, laser micromachining has the distinct advantage of being able to produce high aspect ratio geometries with micron, or several micron, resolution. In addition, the laser process is applicable to a broad range of materials and the laser wavelength can be modified to insure optimum coupling of the laser radiation to the material being machined. The laser process also has a faster process time and is relatively cheaper for use in the development of a conceptual micro device.

Nd:YAG (Neodymium: Yttrium Aluminum Garnet) laser technology is being utilized for rapid prototyping. Unlike excimer lasers that are expensive and have potential environmental, safety, and health concerns due to the toxic gases used, the Nd:YAG laser is more cost effective to acquire and to operate. Moreover, the Nd:YAG laser will allow the operational wavelength to be converted to several frequencies from the near infrared portion of the spectra to the ultraviolet portion of the spectra, using crystal frequency multipliers.

The Nd:YAG laser system has been used successfully to process silicon of varying thicknesses, hole diameters, and geometries (Wong, 1996). Initially, all micropump work was accomplished at the fundamental wavelength (λ) of 1064 nm. Creation of through holes in the silicon (Si) at the wavelength of 1064 nm is done largely by melting and vaporizing the silicon. Most of the fabrication done on the micropump uses this wavelength (1064 nm) for a quick turn-around time.

DESIGN OF AN EHD INJECTION PUMP

Design Requirements

Designing and fabricating a micropump for microelectronic applications is a challenging task. The design requirement for cooling is to extract heat from the hot spot region in a multiple-chip module at about 30 watt/cm^2. This requires the volumetric flow rate in a microchannel to be on the order of 3 milliliters per minute. Several existing micro and conventional pump designs have been investigated. These include membrane pumps (Van Lintel 1988, Miyazaki 1991, Zengerle 1992) as well as pumps without moving parts (Bart 1990, Fuhr 1992, Richter 1990 and 1991). Most pump designs can achieve a pumping rate of several tenths of a *milli*liter per minute but only a few designs can reach a pumping rate of *milli*liters per minute.

Electrohydrodynamic Principle

One fluid pump design that is very attractive in theory is an electrohydrodynamic injection pump, also known as an ion drag pump. The principle behind the ion drag pump is as follows: consider two screen electrodes placed at a fixed distance apart inside a rectangular conduit with an insulating wall (Fig. 1). When an electrical potential is applied to the electrodes, charged particles are uniformly injected into a nonconductive fluid at the upstream electrode (x=0) and then collected at the downstream electrode (x=L). These charged particles are ions generated by a corona discharge. The motion of these charged particles, as they are traveling between the electrodes, will drag the fluid molecules along, thus creating a pumping motion.

DISCLAIMER

Next in this section, we will derive a simple model to illustrate the interaction between the electric field and the induced flow. Interested readers should refer to Melcher (1981) for more detailed information on electromechanics.

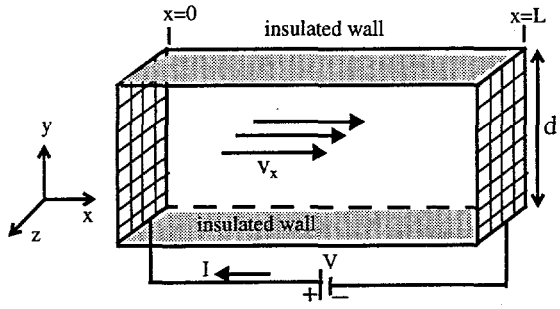

Figure 2 Illustration of the Electrohydrodynamic Principle.

The current density, J_x, associated with the ions discharge and fluid motion in the x-direction is as follows:

$$J_x = \rho_i \cdot (b \cdot E_x + v_x) \tag{1}$$

The first term corresponds to the current generated from the charged particles motion relative to the air. The second term corresponds to the current generated from the induced fluid motion. To simplify our analysis, we will neglect the diffusion and generation of charged particles in the fluid. If we assume that the electric field induced by charges in the fluid is relatively small compared to the electric field imposed by means of the electrodes,

$$E \approx E_o \cdot \hat{e}_x = \frac{V}{L} \cdot \hat{e}_x \tag{2}$$

This implies that for a constant applied voltage, the E field will increase with a decreasing separation distance.

To simplify this analysis, we will only consider a fully developed flow in the x-direction and the flow field is invariant in the z-direction. Hence we can treat the problem as a one-dimensional problem. The general solutions are of the form:

$$\hat{v} = v_x(y) \cdot \hat{e}_x \qquad \rho_i = \rho_i(y) \tag{3}$$

$$\hat{J} = J_x(y) \cdot \hat{e}_x \qquad \frac{\partial P}{\partial x} = constant$$

This general solutions will satisfy the required governing equation which is the x-component of the Navier-Stokes equation.

$$\frac{\partial P}{\partial x} = \rho_i \cdot E_o + \mu \cdot \frac{\partial^2 v_x}{\partial y^2} \tag{4}$$

The current density, J_x, usually varies in the y-direction and can be determined at the inlet. However we can approximate the variation is relatively small and negligible, thus $J_x = J_o$ and is uniform over the cross section. From Eq. (1), we can solve for the charged particle density, ρ_i, and substitute into Eq. (4) to obtain a differential equation for the velocity profile:

$$\frac{\partial P}{\partial x} = \frac{J_o \cdot E_o}{(bE_o + v_x)} + \mu \cdot \frac{\partial^2 v_x}{\partial y^2} \tag{5}$$

The nonlinear expression in Eq. (5) can be reduced to a linear term by restricting attention to circumstances when $bE_o >> v_x$ so that $(bE_o + v_x)^{-1} \cong (bE_o)^{-1} - v_x(bE_o)^{-2}$. Then Eq. (5) can be written as a linear ordinary differential with spatial varying coefficients:

$$\frac{\partial P}{\partial x} = \frac{J_o}{b} - \frac{J_o \cdot v_x}{b^2 \cdot E_o} + \mu \cdot \frac{\partial^2 v_x}{\partial y^2} \tag{6}$$

Equation (6) can be re-arranged as:

$$\frac{d^2 v_x}{dy^2} - \kappa^2 \cdot v_x = -\eta \tag{7}$$

where

$$\kappa = \sqrt{\frac{J_o}{\mu b^2 E_o}} \tag{8}$$

and

$$\eta = \frac{1}{\mu} \cdot \left(\frac{J_o}{b} - \frac{dP}{dx}\right) \tag{9}$$

The boundary conditions are:

at y= 0, $v_x = 0$

at y= d, $v_x = 0$

Hence the solution for the fluid velocity field is as follows:

$$v_x(y) = \frac{1}{\kappa^2} \cdot \eta \cdot \frac{\sinh \kappa d - \sinh \kappa y - \sinh \kappa (d - y)}{\sinh \kappa d} \tag{10}$$

Since the electric Hartman number, H_e, is defined as: $H_e = \sqrt{\frac{J_o d^2}{\mu b^2 E_o}}$, we can express Eq. (10) as:

$$v_x(y) = \left(\frac{d}{H_e}\right)^2 \cdot \frac{1}{\mu} \cdot \left(\frac{J_o}{b} - \frac{dP}{dx}\right) \cdot \frac{\sinh H_e - \sinh H_e\left(\frac{y}{d}\right) - \sinh H_e\left(1 - \frac{y}{d}\right)}{\sinh H_e} \tag{11}$$

The pump characteristic is obtained by integrating Eq. (11) over the channel cross section (where d is the height and w is the width) and the volumetric flow rate, Q_v, will be:

$$Q_v = V_{avg} \cdot d \cdot w \tag{12}$$

where

$$V_{avg} = \left(\frac{d}{H_e}\right)^2 \cdot \frac{1}{\mu} \cdot \left(\frac{J_o}{b} - \frac{dP}{dx}\right) \cdot \left(1 - \frac{2 \cdot (\cosh H_e - 1)}{H_e \cdot \sinh H_e}\right) \quad (13)$$

The last term in Eq. (13) is always smaller than 1 for different electric Hartman number, H_e. Its value spans from 0.0008 for H_e=0.1 to 0.98 for H_e=100. Hence the average fluid velocity with respect to pumping mostly depends on the square of the ratio, d/H_e. This implies:

$$V_{avg} \propto (\mu b^2 E_o)/J_o \quad (14)$$

As the separation distance between electrodes decreases, for a constant applied voltage, the E_o field will increase (Eq. 2) and so does the average fluid velocity (Eq. 14). This analysis illustrates why micro electrohydrodynamic pump is very attractive for our integrated system.

First Design Iteration: A Stacked Geometry

The first electrohydrodynamic pump design uses two stacked silicon wells which are laser drilled to form a grid of holes, and metallized on one side for electrical contact (Fig. 3). Each of the "wells" acts as an electrode and fluid flows vertically between the two plates via the grid of holes in each of the "wells." The wells are formed with a KOH etching process, and then drilled from the well side to create a grid structure of holes. Hole sizes for the grid are about 76 μm to 102 μm in diameter and are spaced about 203 μm to 254 μm apart (Figs. 4 and 5). Well dimensions are 4.57 mm x 3.81 mm and 229 μm deep. Some other pieces were made slightly deeper at 305 μm deep. The bottom part is 8.64 mm x 8.64 mm and the top part is 7.87 mm x 8.64 mm to allow room at the edge for wire bonding. Staystik 383, a nonconductive thermoplastic, is used to join the top and bottom parts along the well perimeters. Using the same Staystik adhesive, the assembled unit is mounted into a 40 pin DIP (Dual-Inline Package) that has a 3.81 mm diameter hole laser drilled through the bottom of the package cavity (Fig. 4). Gold ribbon wire approximately 508 μm x 25 μm is tacked onto the EHD pump electrodes and connected to package leads. Polyimide (MicroSi 115) and Staystik 383 are used to fill the package cavity and to coat the wire bonds. This isolates the wires and metal layers to prevent shorting through the fluid at higher voltages. Shorting was observed as the failure mechanism of uninsulated pumps. Wires are also attached to opposite sides of the package to eliminate shorting between wires.

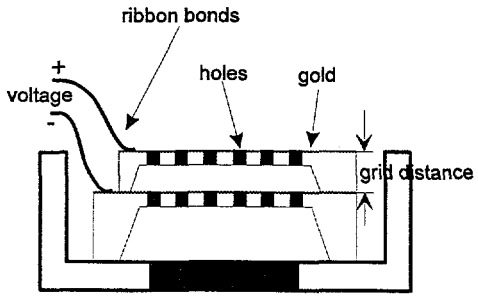

Figure 3 Cross Sectional Diagram of the Stacked Geometry Injection Pump.

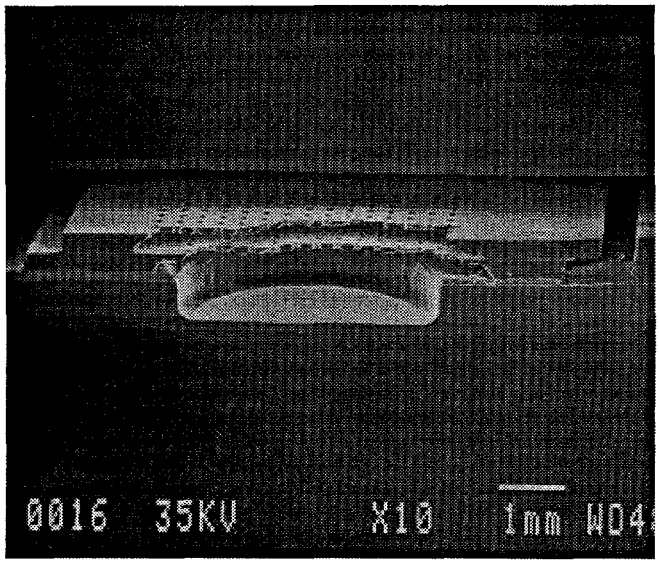

Figure 4 Cross Sectional Photograph of the Assembled Stacked Geometry Injection Pump.

Since relatively lower voltages can be used to obtain effective pumping if the grid distance between the electrode plates (Fig. 3) is reduced, several pumps were constructed with a thinner top part (with thicknesses of 153 μm and 102 μm). This reduces the grid distance from 330 μm to 178 μm and 127 μm, respectively. Grid distance is equal to the top part thickness plus approximately 25 μm for the adhesive layer.

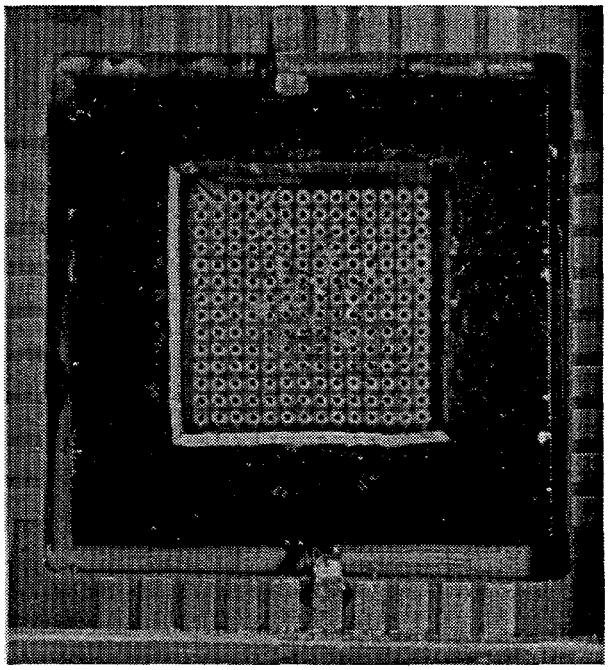

Figure 5 Top View Photograph of the Assembled Stacked Injection Pump.

Next these stacked micro-EHD-pumps were tested and evaluated for their performance. The working fluid being used for the tests is propanol, an organic solvent or alcohol. Preliminary test results show that these micropumps can pump fluid and produce a pressure head. The design with 102 μm holes and a 152 μm grid distance demonstrates that pumping starts at an voltage level of about 60 volts, which is consistent with other electrohydrodynamic micropump designs. More discussion of the testing and evaluation will appear in the following sections.

Second Design Iteration: A Back-to-Back Geometry

The goal of this back-to-back design was to minimize the grid distance between the electrode plates and reduce the corresponding operational voltage. In this design, the same drilled and metallized silicon well pieces were used as in the first iteration except that both the top and bottom parts had 7.87 mm x 8.64 mm dimensions. The metallized portions were mounted toward each other, separated by a layer of nonconductive Stayform adhesive. The Stayform was cut to dimensions of 7.37 mm x 8.64 mm (with a window in the grid region to allow fluid flow) and attached to the parts as illustrated in Figure 6. However during assembly, the Stayform thickness is not consistent such that the grid distance may vary with different devices.

Initially, a layer of Stayform was placed between the parts prior to drilling, but laser drilling through both the silicon and adhesive caused cracking of the part around the exit holes. However, drilling the silicon alone produced clean holes with no observable cracking. The only drawback was that it required some effort to align the holes.

After the pump was assembled, one end of the gold wire was attached to the top part, and the unit was then turned over and attached to the package with Staystik. The other end of the wire was then attached to the package, and the second wire was bonded as usual. Testing and evaluation was also performed on this pump design.

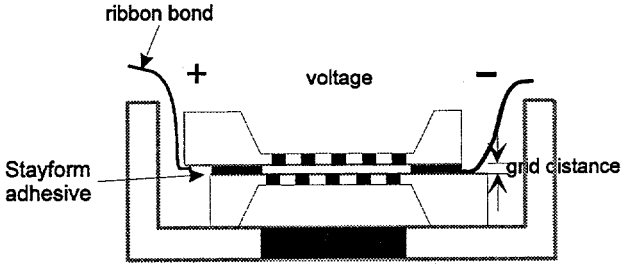

Figure 6 Cross Sectional Diagram of the Back-to-Back Geometry for the EHD Injection Pump.

RESULTS FROM EHD INJECTION PUMP EXPERIMENTS

Setup of the Micropump Experiment

We will present the test results of experimental measurements conducted using a micropump with the "back-to-back" design. This EHD micropump has a 102 μm grid size, 102 μm grid spacing, and as low as 50 μm grid distance. Data collected during the experiments

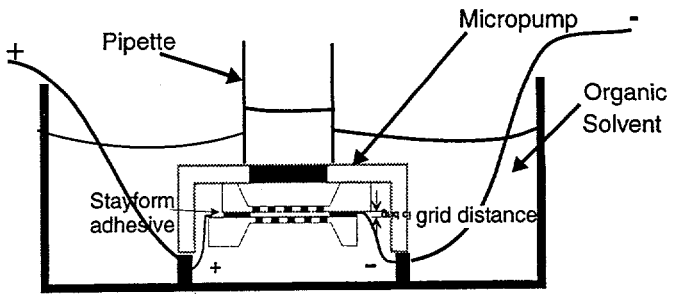

Figure 7 Hardware Setup for the Micro-Electrohydrodynamic Injection Pump Experiments.

included measurement of the established pressure head (measured on a calibrated glass pipette) as a function of the applied electrical voltage. The voltage was applied to the two electrode plates via a standard power supply and the level of voltage was read from a gage affixed to the front of the power supply assembly. Figure 7 shows a schematic diagram of the experimental setup and test equipment used to measure the static pressure in the micro-electrohydrodynamic injection pump during operation. The working fluid used in the EHD pump during these experiments was propanol.

Experimental Results

In this static pressure test, an electrical voltage is applied across the electrodes to induce flow of the propanol through the holes of the two electrode plates. Recall that the voltage differential between the anode plate and the cathode plate induces a flow of ions in the space between and these ions tend to drag fluid molecules along with them. This shearing of fluid molecules then results in a net movement of fluid from one plate to another through the grid of holes drilled in each plate.

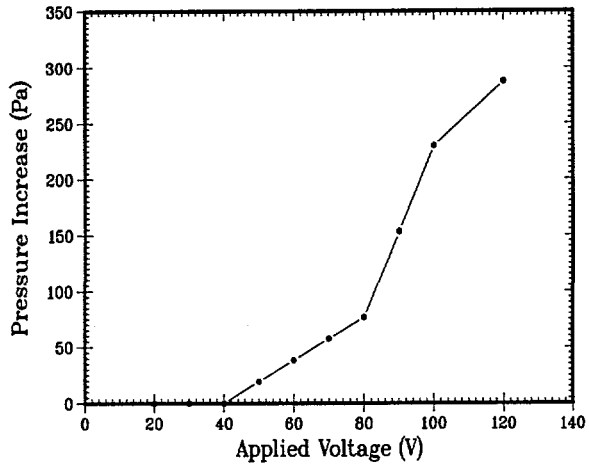

Figure 8 Induced Pressure as a Function of Applied Voltage (EHD Pump: "Back-to-Back," 102 μm Grid Size and Spacing).

Since our major objective during the experiment is to measure the rise in pressure (represented by a corresponding rise in level of the fluid in the glass pipette, or static pressure "head") that the micropump generates with different voltages, a graduated glass pipette was bonded to the outlet of the micropump unit and thus enabled observation of the rise of the liquid level with different applied voltages. Figure 8 plots the induced pressure head as a function of the applied voltage. No liquid level rise is observed until the applied voltage is above approximately 40 volts. Between 50 volts and up to 120 volts, the pressure increases from 19 Pa to 287 Pa. This is consistent with Richter's experiment. The measured pressure head of 287 Pa implies that this micropump is capable to produce a volumetric flow rate of about 2.5 milliliters per minute across a square microchannel of 1 cm long with a 100 μm x 100 μm cross-sectional area.

DISCUSSIONS ON RECENT DEVELOPMENT

At present, we are developing and testing the 3rd iteration of the micro EHD pump. In this design, a thinned Si spacer was used to maintain consistent grid distance between plates. Different spacer thicknesses are being investigated to minimize the voltage required for pumping action. Polyimide was the adhesive used to glue every thing together. The stayform adhesive in the 2nd iteration design gave inconsistent results. This was due to the stayform not providing an even coating for the separation.

Figure 9 shows the results of a modified micropump with a grid distance of ~150 μm. Input power measurement indicates that the micropump required 1 Watt of power to produce 50 Pa of pressure using propanol (uncertainty in the pressure measurement is about 4 Pa). Above 80 volts, gas bubbles began to form on the electrode surface. This could explain the apparent dependence of pressure on the direction of voltage change.

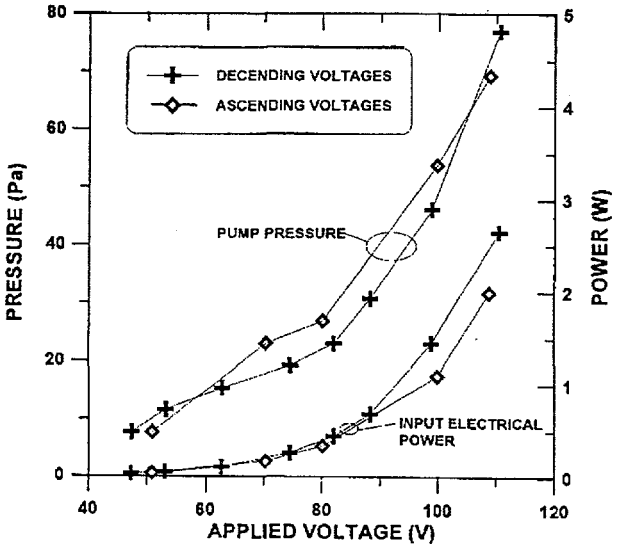

Figure 9 Induced Pressure and Power Input as a Function of Applied Voltage of a Micropump (from the 3rd Design Iteration; Grid Distance~153 μm).

CONCLUSIONS AND RECOMMENDATIONS

As part of a project aimed at determining how micro devices can be integrated into a complete system, an electrohydrodynamic injection micropump was developed using a laser micromachining technology. The EHD micropump successfully demonstrated its ability to generate a flow of propanol based on an applied voltage. Our goal is to rapidly prototype and test single components so that we can speed up the development-to-production cycle. The eventual system to be developed will be an active built-in cooling system for microelectronics applications. Two designs have been investigated. The first design has the silicon parts stacked on top of each other and the second design has the silicon parts bonded back-to-back. A Nd:YAG laser is used to drill an array of circular holes in the well region of both silicon parts, leaving an open pathway for fluid movement. Preliminary results show that the second design with a small grid distance generates a higher pressure head than the stacked design. For the micropump bonded 'back-to-back' with approximately 50 μm spacing, an induced pumping pressure head of 287 Pa was achieved with an application of 120 volts.

REFERENCES

Bart, S. F., Tavrow, L. S., Mehregany, M., and Lang, J. H., 1990, "Microfabricated electrodydrodynamic pumps," *Sensors and Actuators, A. Physical*, Vol. A21-23, pp. 193-197.

Fuhr, G., et al., 1992, "Microfabricated electrohydrodynamic (EHD) pumps for liquid of higher conductivity," *Journal of Micro-ElectroMechanical Systems*, Vol. 1, No. 3, pp. 141-146.

Melcher, J. R., 1981, *Continuum Electromechanics*, MIT Press, Cambridge, Massachusetts.

Miyazaki, S., Kawai, T., and Araragi, M., 1991, "A piezo-electric pump driven by a flexural progressive wave," *Proceedings of IEEE MicroElectroMechanical Systems*, Nara, Japan, pp. 283-288.

Richter, A., and Sandmaier, H., 1990, "An electrodydrodynamic micropump," *Proceedings of IEEE MicroElectroMechanical Systems*, Napa Valley, California, pp. 99-104.

Richter, A., et al., 1991, "Electrohydrodynamic pumping and flow measurement," *Proceedings of IEEE MicroElectroMechanical Systems*, Nara, Japan, pp. 271-276.

Van Lintel, H. T. G., Van De Pol, F. C. M., and Bouwstra, S., 1988, "A piezoelectric micropump based on micromachining of silicon," *Sensors and Actuators*, Vol. 15, pp. 153-167.

Wong, C. C., et al., 1996, "Rapid prototyping of a micro pump with laser micromachining," *SAND Report*, Sandia National Laboratories, Albuquerque, New Mexico.

Zengerle, R., Richter, A., and Sandmaier, H., 1992, "A micro membrane pump with electrostatic actuation," *Proceedings of IEEE MicroElectroMechanical Systems*, Travemunde, Germany, pp. 19-24.

ACKNOWLEDGMENTS

The authors would like to acknowledge Sally L. Liu and Melanie R. Tuck for design and fabrication of the micropump and Simone Smith, John White, and Nao Moore for assisting the construction of the micropump. Many thanks to Zahid Mahmud, John Henfling, and Vincent Amatucci for helping out the micro pump experiment and Anthony Russo and Wayne Trott for their review and comments.